Direct Proof of Endo-Epicardial Asynchrony of the Atrial Wall During Atrial Fibrillation in Humans

Natasja de Groot
Lisette van der Does
Ameeta Yaksh
Eva Lanters
Christophe Teuwen
Paul Knops
Pieter van de Woestijne
Jos Bekkers
Charles Kik
Ad Bogers
Maurits Allessie

ABSTRACT

Background: The presence of focal fibrillation waves during atrial fibrillation (AF) can, beside ectopic activity, also be explained by asynchronous activation of the atrial endo- and epicardial layer and transmurally propagating fibrillation waves. In order to provide direct proof of endo-epicardial asynchrony, we performed simultaneous high-resolution mapping of the right atrial endo- and epicardial wall during AF in humans.

Methods: Intraoperative mapping of the endo- and epicardial right atrial wall was performed during (induced) AF in 10 patients with AF (paroxysmal: N=3, persistent: N=4, longstanding persistent: N=3) and 4 patients without a history of AF. A clamp made of two rectangular 8x16 electrode arrays (interelectrode distance 2 mm) was inserted into the incision in the right atrial appendage. Recordings of 10 seconds of AF were analyzed to determine the incidence of asynchronous endo-epicardial activation times (≥15 ms) of opposite electrodes.

Results: Asynchronous endo-epicardial activation ranged between 0.9-55.9% without preference for either side. Focal waves appeared equally frequent at endocardium and epicardium (11% vs 13%, *P*=0.18). Using strict criteria for breakthrough (presence of an opposite wave within 4 mm and ≤14 ms before the origin of the focal wave), the majority (65%) of all focal fibrillation waves could be attributed to endo-epicardial excitation.

Conclusions: We provided the first evidence for asynchronous activation of the endo-epicardial wall during AF in humans. Endo-epicardial asynchrony may play a major role in the pathophysiology of AF and may offer an explanation why in some patients therapy fails.

INTRODUCTION

Epicardial high density mapping in patients with AF and valvular heart disease has demonstrated that a considerable portion of fibrillation waves showed a focal spread of activation.[1] These focal waves were rarely repetitive and mainly appeared as solitary events. They could occur virtually everywhere in the atria and their coupling interval was often longer than the dominant AF cycle length. In addition, unipolar electrograms recorded at the origin of focal waves, exhibited small R-waves. Based on this indirect evidence, it was postulated that fibrillation waves with a focal pattern of activation could result from endo-epicardial breakthrough (EEB).[1] Since EEBs can only occur in the presence of electrical asynchrony between the endo- and epicardial layer, we hypothesized that the substrate of AF consists of layers of dissociated fibrillation waves that constantly 'feed' each other.[1] In order to demonstrate that endo-epicardial asynchrony (EEA) exists during AF, we performed simultaneous high-resolution, mapping of the endo- and epicardial wall of the right atrium in patients with or without a history of AF undergoing cardiac surgery for coronary artery disease and/or valvular heart disease.

METHODS

Study population

The study sample consisted of 14 patients (10 male, 67±8.3 years) without a history of AF (N=4) and with a history of AF (N=10). Surgical procedures that were performed included cardiac coronary bypass surgery (N=9), mitral valve surgery (N=7), aortic valve replacement (N=2) and tricuspid valve surgery (N=4). Three patients had paroxysmal AF, 4 persistent AF and 3 had persistent AF lasting longer than a year (LSPAF). Atrial enlargement was present in 5 patients. Clinical characteristics of the study population are provided in Table 1.

The mapping protocol was approved by the institutional ethical committee (MEC2010-054) and written informed consent was obtained from all patients prior to the surgical procedure. This study adhered to the declaration of Helsinki principles.

Intraoperative mapping procedure

The mapping study was performed immediately after sternotomy. Following heparinization and arterial cannulation, a temporary bipolar epicardial pacemaker wire was stitched to the right atrial free wall and served as a temporal reference electrode. The indifferent electrode consisted of a steel wire fixed to subcutaneous tissue of the thoracic cavity. If patients were in sinus rhythm at the onset of the mapping procedure, AF was induced by fixed rate pacing at the right atrial free wall using an additional temporary bipolar pacing

wire. The induction protocol started at a rate of 200 beats per minute (bpm). If induction was not successful after 3 burst attempts, the rate was increased by 50 bpm, up to maximal 400 bpm until AF occurred or atrial refractoriness was reached.

Table 1. Clinical characteristics

ID no.	Age (y)	Gender	History of AF	Cardiac surgery	LVF	Atrial dimension
1	65	M	No AF	CABG	good	normal
2	56	M	Persistent	MVP+TVP	good	normal
3	82	M	No AF	CABG	good	normal
4	53	M	Persistent	CABG	poor	RA enlargement
5	66	M	Persistent	MVP+AVR	moderate	LA+RA enlargement
6	80	M	Paroxysmal	CABG+MVP	good	normal
7	63	F	No AF	CABG	good	normal
8	67	M	No AF	CABG	good	normal
9	75	F	LSPAF	MVP+TVP	good	LA+RA enlargement
10	59	M	Persistent	CABG	moderate	normal
11	64	F	LSPAF	MVP+TVP	good	LA enlargement
12	64	M	Paroxysmal	CABG+AVR	good	normal
13	70	F	LSPAF	MVP+TVP	good	LA+RA enlargement
14	71	M	Paroxysmal	CABG+MVP	moderate	normal

M = male; F = female; AF = atrial fibrillation; LSPAF = longstanding persistent atrial fibrillation; CABG = coronary artery bypass grafting; MVP/R = mitral valve plasty/ replacement; TVP = tricuspid valve plasty; AVR = aortic valve replacement; LVF = left ventricular function; RA = right atrium; LA = left atrium.

Prior to commencement to extra-corporal circulation, a high-resolution endo-epicardial mapping clamp was introduced through the right atrial incision for the venous cannula and closed with a purse-string suture. The mapping device was positioned towards the crista terminalis and consisted of two identical rectangular electrode arrays of 8x16 electrodes (interelectrode distance 2 mm) positioned opposite to each other (Figure 1). The electrode arrays (GS Swiss PCB AG, Küssnacht, Switzerland) consist of an electroless nickel immersion gold (ENIG) plated electrode array, mounted on a thin, flexible DuPont™ Pyralux® copper-clad (25 µm thickness) polyimide laminate, and coverlay composite (25 µm) film (0.18 mm). As the space constant of the atrial myocardium is ≈2 mm, the effective spatial resolution of 2.0 mm makes it unlikely that narrow fibrillation wavefronts will not be detected.[2]

All recordings were amplified (gain 1000), filtered (bandwidth 0.5-400 Hz), sampled (1 KHz) and analogue to digital converted (16 bits). A calibration signal of 2 mV amplitude and 1000 ms pulse width was stored simultaneously with atrial electrograms on hard disk using a computerized mapping system. After completion of the mapping procedure, AF was terminated by electrical cardioversion or sustained until cardioplegia was conducted, depending on the operators' preference. Ten seconds of AF were recorded from every patient.

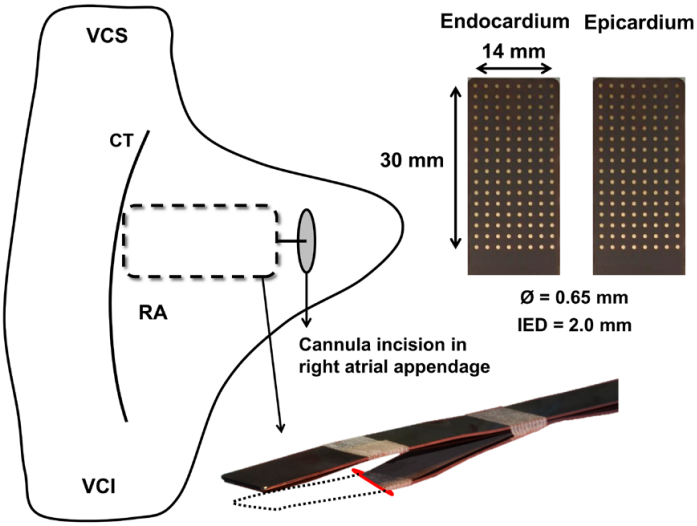

Figure 1. Endo-epicardial mapping device and technique.
The mapping device consists of two rectangular 8x16 electrode arrays with an interelectrode distance (IED) of 2 mm fixed to spatulas and positioned precisely opposite to each other. During endo-epicardial mapping, the endocardial leg is inserted in the right atrium (RA) through the incision of the venous cannula and closed with a purse-string suture. The array is positioned towards the crista terminalis (CT). VCS/VCI, vena cava superior/ inferior.

Mapping data

Series of endo- and epicardial wavemaps of 10 seconds AF were reconstructed from the two sets of 128 unipolar fibrillation electrograms, using custom-made software which has been previously described in detail.[1,3] For every electrode, local activation times were determined by marking the steepest negative deflection of the unipolar fibrillation electrograms. In case of a fractionated potential, the steepest negative deflection was chosen. At every electrode at either the endo- or epicardial layer, differences in endo-epicardial activation times were determined by measuring the smallest time delay within the opposite square base of 3x3 electrodes (Figure 2). The total amount of EEA during the entire recording period was expressed as the percentage of transmural differences of ≥15 ms for all endo- and epicardial recording sites. The combined asynchrony map (lower right panel of Figure 2) shows the longest time delay for every endo-epicardial electrode couple.

Wavemapping was used to identify the individual fibrillation waves. The starting point of the first fibrillation waves was the earliest activated site within the mapping area. Next, the entire mapping area was scanned in steps of 1 ms. For all electrodes activated during every step, the shortest time difference with the 8 neighboring electrodes was calculated. When the time difference was ≤12 ms (17 ms for oblique distances), the electrode site was added

to the territory of the surrounding wave. In case of a time difference >12 ms, the electrode was annotated as the starting point of a new wave. In the wavemap, fibrillation waves are color-coded according to their moment of entrance in the mapping area and the colors demarcate the area activated by that specific fibrillation wave.[4] Wavemaps also identify focal waves at either the endo- or epicardial surface. Focal fibrillation waves had to meet previously defined criteria. The breakthrough site of the focal fibrillation wave had to be located at least 2 electrodes away from the border of the mapping array and at least 1 reliable activation time should be available between the breakthrough site and the border of the mapping area. The morphology of the electrograms in the breakthrough region should not be distorted by large QRS complexes or artifacts. If this is the case, the wave is excluded from analysis. The focal wave should at least cover 4 electrodes. The origin of a focal wave

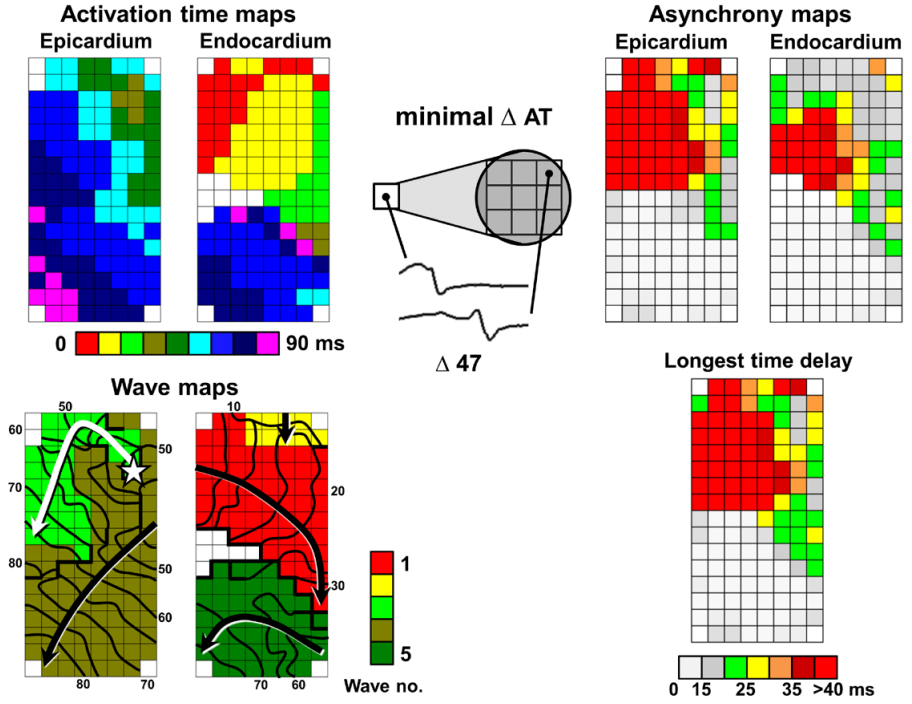

Figure 2. Construction of activation, wave and asynchrony maps.
Activation times determined at each individual electrode of endocardial and epicardial arrays are depicted in color-coded activation maps starting at the time of first activation. Wavemaps are automatically constructed which demonstrate the number and sequence of appearance of different waves activating the mapping area and also illustrate the origin of focal waves beginning within the mapping area (white star). Isochrones are set with intervals of 5 ms and indicate the main trajectory of each wave (black/white arrows). Thick black lines indicate conduction block (Δ≥12 ms). The asynchrony map of either the endocardial or epicardial layer consists of the endo-epicardial activation times defined by the smallest interval of the opposite nine activation times; the total asynchrony map shows the longest time delay assessed at every coupled recording site.

had to be activated earlier than all surrounding electrodes. If electrodes adjacent to the origin were activated simultaneously, all electrodes surrounding this area should also be activated later. Shift of the local activation time to a maximum of 3 ms earlier or later at the earliest activated electrode(s) should not result in disappearance of the focal wave. If a breakthrough site emerged along the border of another fibrillation wave, the time delay between that wave and the origin of the breakthrough had to be at least 40 ms.[1] All these criteria were checked manually by 2 independent investigators. A more detailed description of the mapping criteria with examples is provided in the supplemental material.

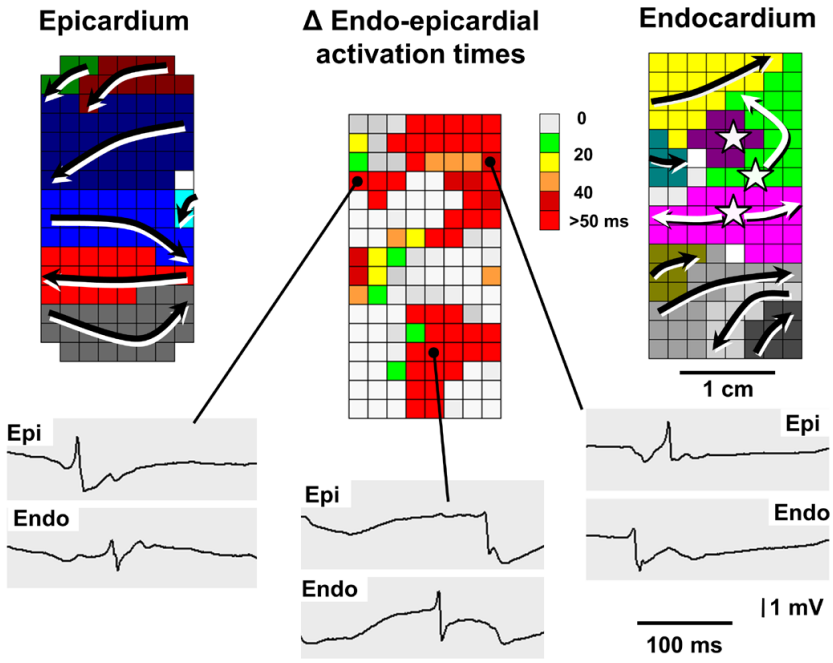

Figure 3. Endo-epicardial asynchrony in a patient with longstanding persistent atrial fibrillation.
The maps represent a single AF-cycle of 190 ms. The left and right panels show simultaneous wavemaps of the sub-epicardium and sub-endocardium of a part of the free wall of the right atrium (3.0 x 1.4 cm). The colors indicate the sequence of appearance of the different fibrillation waves (rainbow scheme followed by a grayscale). The arrows indicate the main trajectories of the waves. The sub-epicardium of the right atrium was activated by 7 narrow fibrillation waves, entering the mapping area from various directions. The endocardium was activated by 9 waves, 3 of them arising as focal waves in the middle of the mapping area (white stars). The local endo-epicardial time-differences are plotted in the central map. As a result of the different activation patterns at the endocardial and epicardial surface, major differences in endo-epicardial activation times existed (up to >50 ms). There was considerable spatial dispersion in EEA, with differences in endo- and epicardial activation times ranging from 0 to >50 ms. The 3 electrogram-pairs at the bottom, clearly show the marked differences in endocardial and epicardial activation times. Sometimes the epicardium was activated earlier (left panel), sometimes the endocardium (middle and right panels).

To assess whether focal fibrillation waves could originate from endo-epicardial breakthrough, in each case the opposite layer was examined for the presence of a fibrillation wave that could have served as a source for the focal wave. The presence of an opposite wavefront, within 4 mm distance and less than 15 ms before the origin of the focal wave, was considered to reflect transmural conduction based on normal atrial conduction properties. In this case, the focal wave could from a theoretically point of view be attributed to endo-epicardial breakthrough.

Statistical analysis

The Wilcoxon signed rank test was performed to assess the occurrence of EEA and focal waves between the epi- and endocardium.

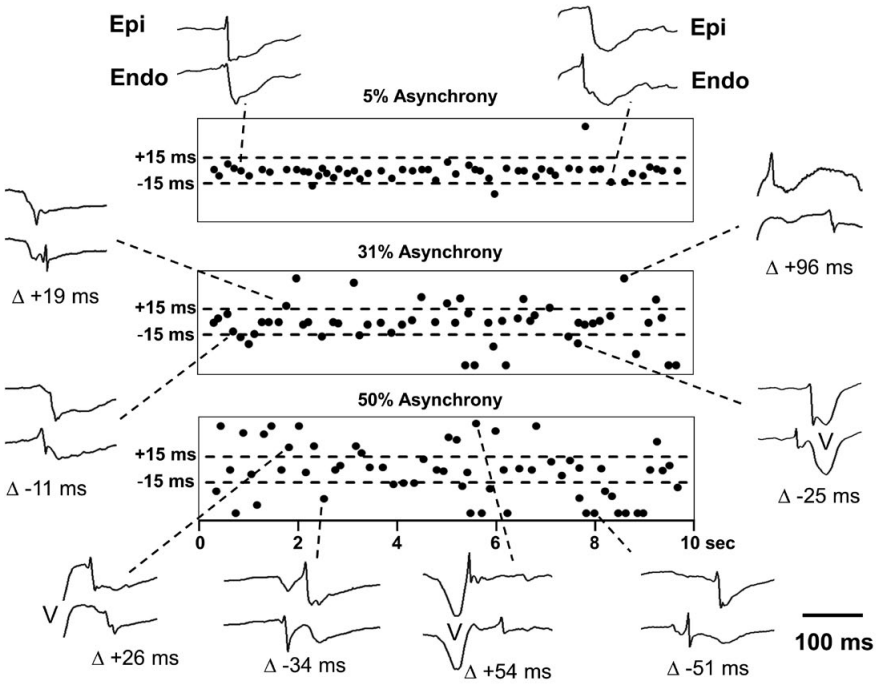

Figure 4. Spatial and temporal variation in endo-epicardial asynchrony during longstanding persistent AF. Endo-epicardial asynchrony plots of 10 seconds of AF, recorded at 3 different locations of the right atrial free wall in a patient with AF. The dashed horizontal lines demarcate the band of endo-epicardial synchrony; data points > ±50 ms are clipped. At different sites, the degree of EEA (delay ≥15 ms) varied from 5% (top panel), 31% (middle) and 50% (bottom). In addition to spatial dispersion, EEA also showed a strong temporal variation. As can be seen from the middle and lower plots, differences in endo-epicardial activation time seemed to occur randomly, without a clear predominance of either the sub-endocardial or sub-epicardial layer. Examples of pairs of unipolar endocardial and epicardial electrograms demonstrating the spatial temporal variation are given around the plots.

RESULTS

Endo-epicardial asynchrony

In the entire study population, the average percentage of missing data due to poor contact of the mapping array was 7.8±4.9%. The amount of conduction block was similar in the epicardial and endocardial plane with incidences of respectively 10.8±5.1% and 10.8±4.6%. Simultaneous epi- and endocardial wavemaps of a single AF-cycle recorded in a patient with longstanding persistent AF demonstrating EEA are shown in Figure 3. In this example, marked differences in activation patterns of the endo- and epicardial wall existed; almost all fibrillation waves at the endo- and epicardial surface appeared at different times and/or propagated in different directions.

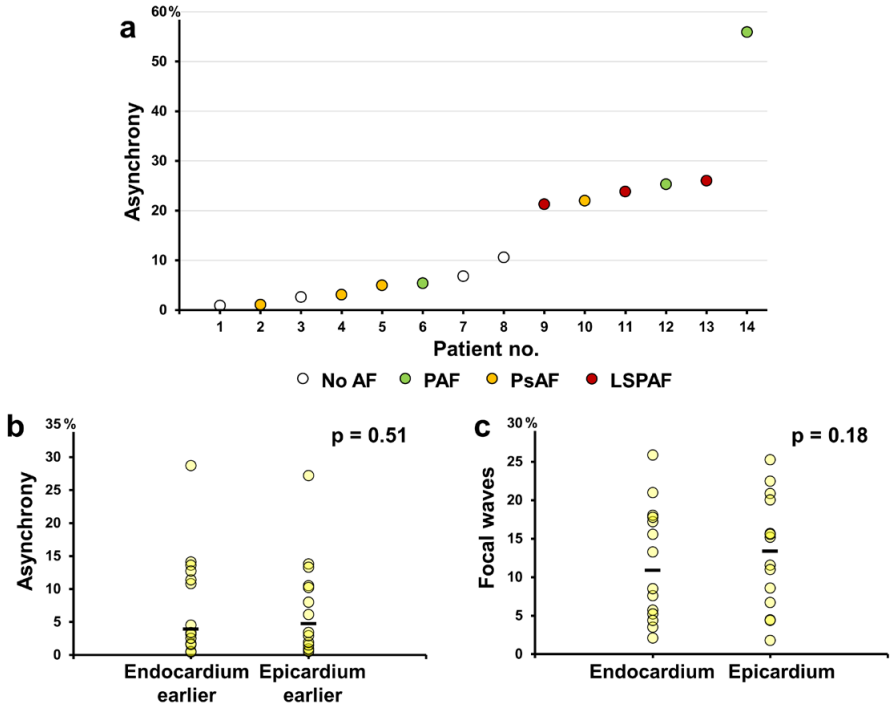

Figure 5. Endo-epicardial asynchrony levels and focal waves.
A: Graph demonstrating the total amount of EEA plotted for every patient separately; patients are ranked according to the degree of EEA. Type of AF (none, paroxysmal, persistent, longstanding persistent) is illustrated by the different grayscale tones. B and C: Dot plots and medians of (b) the incidence of asynchrony where endocardium versus epicardium is activated earlier in respect to the other and (c) the percentage of focal waves (of total number of waves) recorded at the endocardium and epicardium. For both parameters, there was no difference between the endocardial and epicardial layer (*P*=0.51 and *P*=0.18).

Table 2. Endo-epicardial asynchrony and focal waves

ID no.	AFCL (ms)	Endo-epicardial asynchrony (%)	Endocardium earlier (%)	Epicardium earlier (%)	Endo-epicardial activation SD (ms)	Endocardial fibrillation waves			Epicardial fibrillation waves		
						Number waves	Focal	Breakthroughs (% of focal)	Number waves	Focal	Breakthroughs (% of focal)
1	206±28	0.9	0.4	0.5	4.2	115	4	75	112	2	100
2	181±28	1.1	0.5	0.6	4.4	140	8	87	140	12	92
3	175±32	2.6	1.7	0.9	7.7	192	10	60	224	10	80
4	246±28	3.1	1.6	1.5	5.5	186	32	56	187	42	81
5	150±28	5.0	3.1	1.9	8.5	277	21	90	294	34	94
6	182±40	5.4	2.5	2.9	9.4	347	54	81	257	39	92
7	141±24	6.8	3.4	3.4	12.7	239	5	40	251	11	73
8	140±27	10.6	4.5	6.1	12.3	445	59	83	337	37	73
9	147±40	21.3	10.8	10.5	18.2	553	116	66	657	137	55
10	189±40	22.0	14.1	8.0	19.6	494	89	54	470	94	55
11	224±46	23.8	13.6	10.2	23.7	343	61	69	345	54	57
12	189±40	25.3	11.4	13.8	25.4	321	83	55	329	83	59
13	151±35	26.0	12.7	13.3	20.4	480	21	86	372	25	80
14	183±37	55.9	28.7	27.2	37.2	188	16	25	257	40	30
Total/ mean	-	15.0	7.8	7.2	-	4320	579	66	4232	620	65

AFCL = atrial fibrillation cycle length; SD = standard deviation.

In this same patient, the spatio-temporal variation in EEA during 10 seconds of AF is demonstrated in Figure 4. The degree of EEA varied considerably at different locations and at different times. No clear predominance of either the endocardial or the epicardial layer was observed. Examples of unipolar electrogram-pairs around the plots illustrate the high spatio-temporal variation in EEA.

As demonstrated in Figure 5, the total degree of EEA in our study population varied widely between 0.9 and 55.9% and there was no clear difference between endo-epicardial and epi-endocardial asynchrony (respectively 7.8±7.7% and 7.2±7.2%).

Focal fibrillation waves

In total 1199 focal fibrillation waves were observed, 579 arising at the sub-endocardium and 620 at the sub-epicardium. The equal distribution of focal fibrillation waves between both sides is shown in panel C of Figure 5. Applying the previously stated strict criteria for endo-epicardial breakthrough, 784 of all 1199 focal waves (65%) could be attributed to result from endo-epicardial excitation presuming that normal conduction occurs between

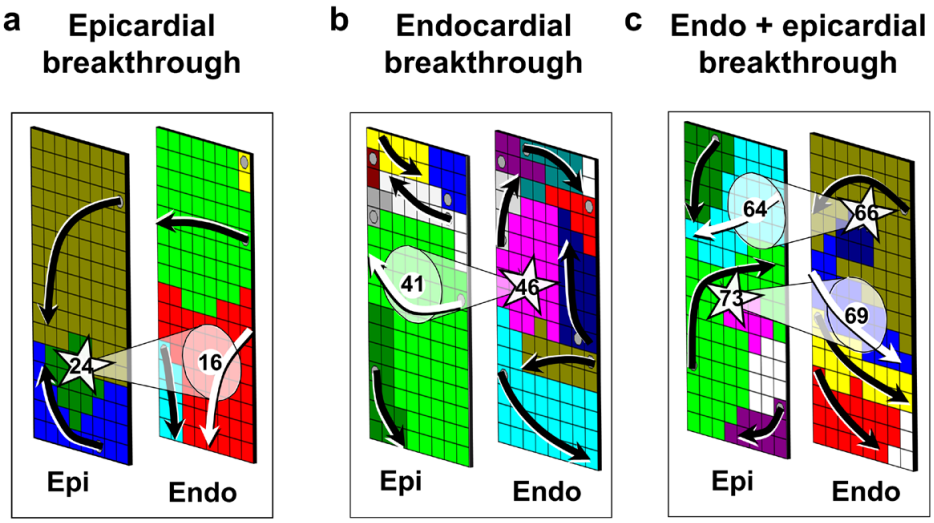

Figure 6. Three examples of endo-epicardial breakthroughs in a patient with longstanding persistent AF. A: A focal wave appeared at the epicardial surface at t=24 (white star). As can be seen from the associated endocardial wavemap, just a couple of milliseconds before an endocardial fibrillation wave (red) had passed that site at t=16 ms. A transmural conduction time of only 8 ms was taken as supportive evidence that the focal wave could be due to endo-epicardial breakthrough. B: An example of a focal wave arising at the endocardium at t=46. Again a fibrillation wave in the opposed layer (green) had passed that site just 5 ms before (at t=41). C: Two breakthroughs occurred at about the same time, one at the endocardium at t=66 and one at the epicardium at t=73 ms. In both cases, in the opposite layer a fibrillation wave passing the site of origin of the focal waves a few ms earlier at respectively t=64 and t=69, indicating that the focal waves could result from endo-epicardial breakthrough.

endo-epicardium (66% of the endocardial and 65% of the epicardial focal waves) (Table 2). Examples of pairs of endo-epicardial wavemaps showing focal fibrillation waves originating from EEB of fibrillation waves from the opposite layer are given in Figure 6.

DISCUSSION

Despite the relatively small number of patients, our data clearly show that a significant degree of EEA is present in the right atrium in patients with AF. Simultaneous endo-epicardial mapping of isolated canine atria, both during sinus rhythm and atrial pacing, only showed small differences in activation times (<1 ms). However, during atrial tachyarrhythmias, activation of the endo- and epicardial layers has been shown to become more asynchronous (up to 25 ms), particularly in the thicker parts of the atria.[5,6] In isolated fibrillating sheep atria, breakthrough sites appeared to be related to sub-endocardial muscle structures, the three-dimensional structure of the atria determining the appearance of focal waves during AF.[7] The concept that endo-epicardial dissociation might play an important role in the maintenance of AF, stems from experimental studies in the goat model of persistent AF.[8-10] These studies showed that the endo- and epicardial layers of the atrial wall became progressively dissociated during the first 6 months of AF. After that time, fibrillation waves in the endo- and epicardial layers often propagated at different speed and in different directions, and endo-epicardial breakthroughs became more abundant.[8,9]

In this study, the incidence of endo-epicardial asynchrony tended to be higher in patients with AF, though we did not observe a clear relation between duration of AF and degree of EEA. This can be explained by the fact that we did not map the left atrium and that if EEA of the left atrial wall also exists, it may play a more important role in the pathophysiology of AF. Also, our study population contained a small number of patients with a variety of cardiac diseases.

We provided additional data that most focal fibrillation waves could be explained by endo-epicardial excitation. Lee et al. also frequently observed focal fibrillation waves without any sustained focal activity in 18 patients with persistent AF.[11] In contrast, low-density mapping studies using a 64-pole basket catheter, have suggested that AF is maintained by a limited number of rapid stable sources (rotors and/or ectopic foci).[12,13] Body surface mapping during AF elucidated the presence of non-sustained re-entries and focal breakthroughs in certain domains of the atria.[14] Recently, we have discussed the discrepancies in the interpretation of high- and low-resolution mapping of AF in detail in a crosstalk paper.[15,16] The present study supports the concept that during AF, the endo- and epicardial layers of the atrial wall can be asynchronously activated.[1,16] The presence of dissociated

layers of fibrillation waves, will highly stabilize the fibrillatory process because, as soon as fibrillation waves die out, they can be replaced by breakthroughs from the opposite side.

In such a substrate, each layer will serve as a multi-site generator for the other layer. During 10 seconds of AF, more than 20-30 focal waves appeared at each side of the atrial wall, in an area of only 2.6 cm.[1] Extrapolating this number to the entire atrial surface, the total number of focal breakthrough waves can be estimated to exceed 10.000 per minute. However, we like to emphasize that the presence of EEA, off course does not disprove that also re-entry and focal activity may contribute to the maintenance of AF. In different stages of the development of a substrate of AF, the contribution of different mechanisms for perpetuation of AF may vary. We fully acknowledge the large body of evidence that re-entrant and focal mechanisms are operative during atrial fibrillation.[17-20] In fact, not all focal fibrillation waves in our patients could be attributed to endo-epicardial breakthrough, and sometimes two focal waves appeared simultaneously at the endo- and epicardial surface. Equally, our data do not rule out the possibility that some of the endo-epicardial breakthroughs formed part of a transmural re-entrant circuit. However, we venture to suggest that progressive, AF induced, structural atrial remodeling gradually transforms the atrial wall into multiple layers of narrow dissociated wavelets. With time, more and more focal breakthroughs will be generated, which progressively stabilizes the fibrillatory process. At the end, the main source of fibrillation waves is formed by an abundant number of focal breakthroughs, occurring virtually everywhere in the atria. This is in agreement with the recent finding of Haïssaguerre et al., that the number of driver regions increased with the duration of AF, until after 6 months almost the entire atrial wall acted as a driver (6 of all 7 regions).[14] It also explains why the termination rate of AF by driver ablation sharply declined after 6 months of AF.[14]

Study limitations

Our study population is presently limited to 14 patients and a larger number of patients is obviously required for a meaningful statistical analysis and to study the relation between persistence of AF and the degree of electrical asynchrony. Expanding the study population will also allow for statements about a possible correlation between EEA and breakthroughs. Moreover, the effective spatial resolution of the recordings is dependent on the number of electrodes with good tissue contact. Another limitation is, that so far, only a limited part of the atria has been accessible for endo-epicardial mapping (4.2 cm^2 of the right atrium). In order to get a full understanding of the role of EEA in the development of the substrate of AF, endo-epicardial mapping of the left atrium is needed as well. However, the left atrium is not standardly opened during cardiac surgery, only during selected procedures. In addition, opening the left atrium before cardiopulmonary bypass is associated with a considerable increase in the risk for air embolism which may cause brain injury. Therefore,

we decided it was not ethically responsible to perform endo-epicardial mapping of the left atrium for this pilot study.

Clinical implications

Knowledge of the substrate and various mechanisms of perpetuation of human AF is of great importance to understand the natural history of AF. At different stages, the substrate of AF may require different treatment modalities. At an early stage pulmonary vein isolation alone might be sufficient, whereas in a later stage also compartmentalization of the atria will be necessary to restore sinus rhythm. Furthermore, when the endo- and epicardial layers of the atria have become electrically dissociated, even extensive ablative therapies may be ineffective and palliative therapy would be a better option. Knowledge of the vulnerable parameter(s) for perpetuation of AF, and the ability to diagnose the stage of development of the substrate of AF, are essential for an individualized and staged therapy of atrial fibrillation.

REFERENCES

1. de Groot NMS, Houben RP, Smeets JL, Boersma E, Schotten U, Schalij MJ, Crijns H, Allessie MA. The electropathological substrate of longstanding persistent atrial fibrillation in patients with structural heart disease: epicardial breakthrough. Circulation. 2010;122:1674-1682.
2. Sakamoto Y, Goto M. A study of the membrane constant in the dog myocardium. Jap J Physiol. 1970;20:30-41.
3. Allessie MA, de Groot NM, Houben RP, Schotten U, Boersma E, Smeets JL, Crijns HJ. The electropathological substrate of longstanding persistent atrial fibrillation in patients with structural heart disease: longitudinal dissociation. Circ Arrhythm Electrophysiol. 2010;3:606-615.
4. Rogers JM, Usui M, KenKnight BH, Ideker RE, Smith WM. Recurrent wavefront morphologies: a method for quantifying the complexity of epicardial activation patterns. Ann Biomed Eng. 1997;25:761-768.
5. Schuessler RB, Kawamoto T, Hand DE, Mitsuno M, Bromberg BI, Cox JL, Boineau JP. Simultaneous epicardial and endocardial activation sequence mapping in the isolated canine right atrium. Circulation. 1993;88:250-263.
6. Derakhchan K, Li D, Courtemanche M, Smith B, Brouillette J, Pagé PL, Nattel S. Method for simultaneous epicardial and endocardial mapping of in vivo canine heart: application to atrial conduction properties and arrhythmia mechanisms. J Cardiovasc Electrophysiol. 2001;12:548-555.
7. Gray RA, Pertsov AM, Jalife J. Incomplete reentry and epicardial breakthrough patterns during atrial fibrillation in the sheep heart. Circulation. 1996;94:2649-2661.
8. Eckstein J, Maesen B, Linz D, Zeemering S, van Hunnik A, Verheule S, Allessie M, Schotten U. Time course and mechanisms of endo-epicardial electrical dissociation during atrial fibrillation in the goat. Cardiovasc Res. 2011;4:816-824.
9. Eckstein J, Zeemering S, Linz D, Maesen B, Verheule S, van Hunnik A, Crijns H, Allessie MA, Schotten U. Transmural conduction is the predominant mechanism of breakthrough during atrial fibrillation: evidence from simultaneous endo-epicardial high-density activation mapping. Circ Arrhythm Electrophysiol. 2012;6:334-341.
10. Verheule S, Eckstein J, Linz D, Maesen B, Bidar E, Gharaviri A, Schotten U. Role of endo-epicardial dissociation of electrical activity and transmural conduction in the development of persistent atrial fibrillation. Progress in Biophysics and Molecular Biology. 2014;115:173-185.
11. Lee G, Kumar S, Teh A, Madry A, Spence S, Larobina M, Goldblatt J, Brown R, Atkinson V, Moten S, Morton JB, Sanders P, Kistler PM, Kalman JM. Epicardial wave mapping in human long-lasting persistent AF: transient rotational circuits, complex wave fronts and disorganized activity. Eur Heart J. 2014;35:86-97.
12. Narayan SM, Krummen DE, Shivkumar K, Clopton P, Rappel WJ, Miller JM. Treatment of atrial fibrillation by the ablation of localized sources: CONFIRM (CONventional ablation for atrial fibrillation with or without Focal Impulse and Rotor Modulation) trial. J Am Coll Cardiol. 2012;60:628-636.
13. Narayan SM, Shivkumar K, Krummen DE, Miller JM, Rappel WJ. Panoramic electrophysiological mapping but not electrogram morphology identifies stable sources for human atrial fibrillation: stable atrial fibrillation rotors and focal sources relate poorly to fractionated electrograms. Circ Arrhythm Electrophysiol. 2013;6:58-67.
14. Haïssaguerre M, Hocini M, Denis A, Shah AJ, Komatsu Y, Yamashita S, Daly M, Amraoui S, Zellerhoff S, Picat MQ, Quotb A, Jesel L, Lim H, Ploux S, Bordachar P, Attuel G, Meillet V, Ritter P, Derval N, Sacher F, Bernus O, Cochet H, Jaïs P, Dubois R. Driver domains in persistent atrial fibrillation. Circulation. 2014;130:530-538.

15. Narayan SM, Jalife J. CrossTalk proposal: Rotors have been demonstrated to drive human atrial fibrillation. J Physiol. 2014;592:3163-3166.
16. Allessie MA and de Groot NM. CrossTalk opposing view: Rotors have not been demonstrated to be the drivers of atrial fibrillation. J Physiol. 2014;592:3167-3170.
17. Andrade J, Khairy P, Dobrev D, Nattel S. The clinical profile and pathophysiology of atrial fibrillation: relationships among clinical features, epidemiology, and mechanisms. Circ Res. 2014;114:1453-1468.
18. Nattel S, Shiroshita-Takeshita A, Brundel BJ, Rivard L. Mechanisms of atrial fibrillation: lessons from animal models. Prog Cardiovasc. Dis. 2005;48:9-28.
19. Schotten U, Verheule S, Kirchhof P, Goette A. Pathophysiological mechanisms of atrial fibrillation: a translational appraisal. Physiol Rev. 2011;91:265–325.
20. Heijman J, Voigt N, Nattel S, Dobrev D. Cellular and molecular electrophysiology of atrial fibrillation initiation, maintenance, and progression. Circ Res. 2014;114:1483-1499.

SUPPLEMENTAL MATERIAL CHAPTER 9: MAPPING CRITERIA

Step I. Subtraction of ventricular complexes

Before determination of the local activation time, ventricular complexes were eliminated from the unipolar electrograms using a subtracting technique as previously described in detail by Hoekstra et al.[1] In short, for each fibrillation electrogram an individual template of the ventricular far field was obtained by averaging all time windows of ±70 ms around the R-waves detected from surface ECG lead I. Subtraction of these individual QRS templates from the fibrillation electrograms reduces the ventricular far field potentials and results in a more or less 'clean' unipolar atrial fibrillation electrograms.

Step II. Determination of the local activation time

Examples of electrograms recorded from both the endo- and epicardium showing endo-epicardial (a)synchrony are demonstrated in Supplemental Figure 1.

Local activation times were determined by detecting the maximum downslope of the unipolar fibrillation potential, as this coincides with the moment of maximum rate of rise of the transmembrane potential (time differences less than 50 μs).[2] In turn, the maximum rate of rise of the transmembrane potential corresponds with the maximum increase in sodium current and its conductance.[3] The height of the negative slope is measured during a 2 ms period. From the moment of the maximum downslope, time windows both backward and forward in time are scanned to detect the moment of respectively the positive and negative peak of the fibrillation potential. The duration of a non-fractionated potential is then defined as the time difference between the moment of its negative and positive peak. In case of a fractionated potential, the deflection with the steepest down slope was chosen; its duration is defined as the time between the preceding positive and following negative deflection.[4] The duration of a fibrillation potential had to be ≤35 ms. The negative slope and amplitude of the unipolar fibrillation potentials depend on numerous variables.[5,6] Hence, cut-off values applied also vary, depending on the signal-to-noise ratios of the recordings and lower limits were set at 0.05 V/sec and 0.2 mV.[5,6,7,8] All fibrillation potentials with slopes <0.05 V/sec, amplitudes < 0.2 mV and durations >35 ms are thus regarded as either far field or poor contact potentials.

After detection of the local activation time, a blanking period of 40 ms was applied in both directions. Though we do not know exactly what the refractory period during AF is, it is estimated to be approximately 50±13 ms.[9] Hence, comparable to previous studies, by choosing a blanking period of 40 ms we avoid overestimation of the number of fibrillation waves by marking fibrillation potentials, which are most likely double potentials with interspike intervals between >0 and ≤40 ms caused by areas of conduction block. [10,11]

Step III. WaveMapping

A wavemapping approach was used to identify individual fibrillation waves. This wavemapping technique has also been described in prior studies.[2,3,12,13] The starting point of the first fibrillation waves was the earliest activated site within the mapping area. Next, the entire mapping area was scanned in steps of 1 ms. For all electrodes activated during every step, the shortest time difference with the 8 neighboring electrodes was calculated. When the time difference was ≤12 ms (17 ms for oblique distances), the electrode site was added to the territory of the surrounding wave. In case of a time difference >12 ms, the electrode was annotated as the starting point of a new wave. In the wavemap, fibrillation waves are color-coded according to their moment of entrance in the mapping area and the colors demarcate the area activated by that specific fibrillation wave. The cut-off value of >12ms used for separating individual fibrillation waves corresponds for 2 mm interelectrode distances with an effective conduction velocity of 17 cm/s, which is equivalent to the continuous conduction velocities reported for atrial myocardium of intact hearts.[14] For separation of the fibrillation waves the requirement of a lower limit CV must be fulfilled along the whole boundary of the wave which off course does not exclude the possibility of slow conduction within parts of the fibrillation waves. Choosing a different cut-off value will lead to a lower or higher number of fibrillation waves. However, this change is very gradual and has no major effects on the measured differences in the number of focal waves. Only at extreme cut-off values our analysis will become useless because it either no longer separates the different fibrillation waves, or results in a very high degree of spatial fractionation, resembling a mosaic-like pattern of numerous small waves that only propagate over very short distances.

Based on the origin of the fibrillation wave, three different types of fibrillation waves were distinguished 1) peripheral waves, entering the mapping area from outside the electrode array, 2) epicardial breakthrough, appearing at the epicardial surface inside the mapping area, and 3) discontinuous conduction waves; defined as fibrillation waves starting with a delay of 13 to 40 ms from the boundary of another wave.[12-13] If a fibrillation wave originates along the border of another fibrillation wave it could theoretically be the result of very slow conduction. In order to avoid overestimation of the number of focal waves, we classified these waves as discontinuous fibrillation waves. Applications of this wavemapping technology have been described previously.[12-13]

Focal fibrillation waves had to meet several criteria. The breakthrough site of the focal fibrillation wave had to be located at least 2 electrodes away from the border of the mapping array and at least 1 reliable activation time should be available between the breakthrough site and the border of the mapping area in order to exclude propagation from the border of the mapping array. An example is given in Supplemental Figure 2. The relation between

the percentage of endocardial or epicardial focal fibrillation waves and the distance from the origin of the focal wave to the border of the mapping array is shown in Supplemental Table 1. Next, it is manually checked whether the morphology of fibrillation potentials in the breakthrough region is distorted by large QRS complexes or artifacts due to e.g. movements of the electrodes in order to avoid false positive focal waves; examples are shown in Supplemental Figure 3.

In case of a fractionated electrogram, marking of one of the other deflections should not result in disappearance of the focal fibrillation wave (Supplemental Figure 4). In order to include only focal waves which have a more or less considerable impact on endo-epicardial asynchrony, we choose cut-off value of 4 electrodes. Supplemental Table 2 shows how many focal waves will disappear when a cut-off value of 5 or 6 electrodes would have been chosen. The origin of a focal wave had to be activated earlier than all surrounding electrodes. If electrodes adjacent to the origin were activated simultaneously, all electrodes surrounding this area should also be activated later. Shift of the local activation time to a maximum of 3 ms earlier or later at the earliest activated electrode(s) should not result in disappearance of the focal wave. Typical examples of focal waves resulting from these criteria are provided in Supplemental Figure 5.

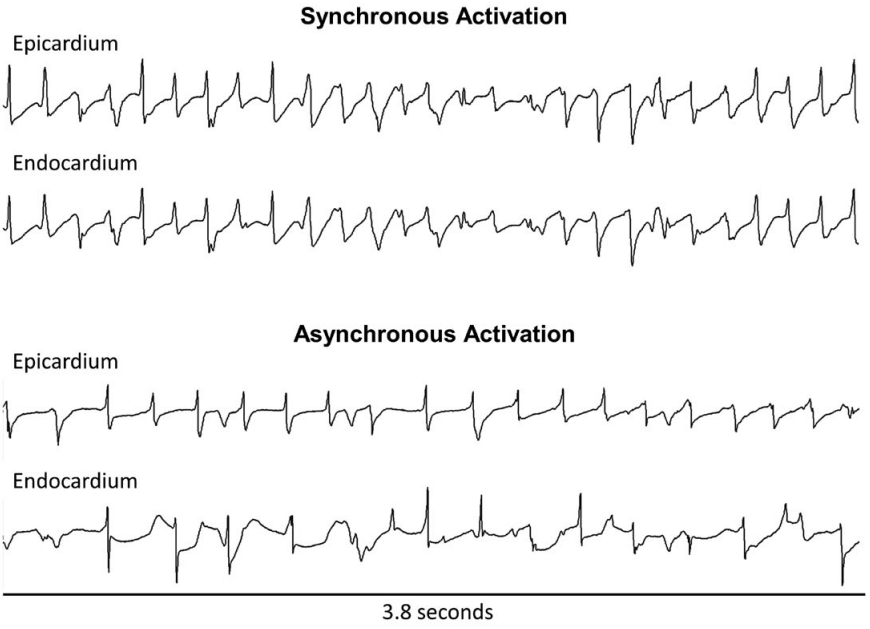

Supplemental Figure 1. Examples of two opposite electrogram recordings showing synchronous and asynchronous activation.

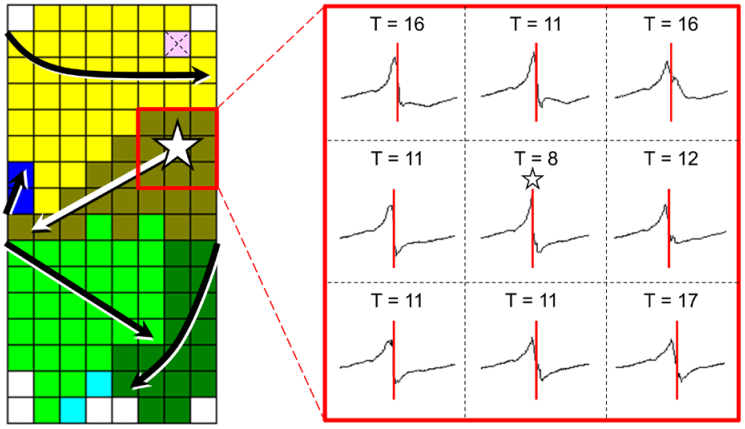

Supplemental Figure 2. Focal wave originating near the border of the mapping array.

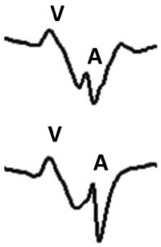

Supplemental Figure 3. Distortion of the morphology of an atrial fibrillation potential by a far field ventricular complex.

Supplemental Figure 4. Fractionated potential next to the origin of a 'focal' wave.

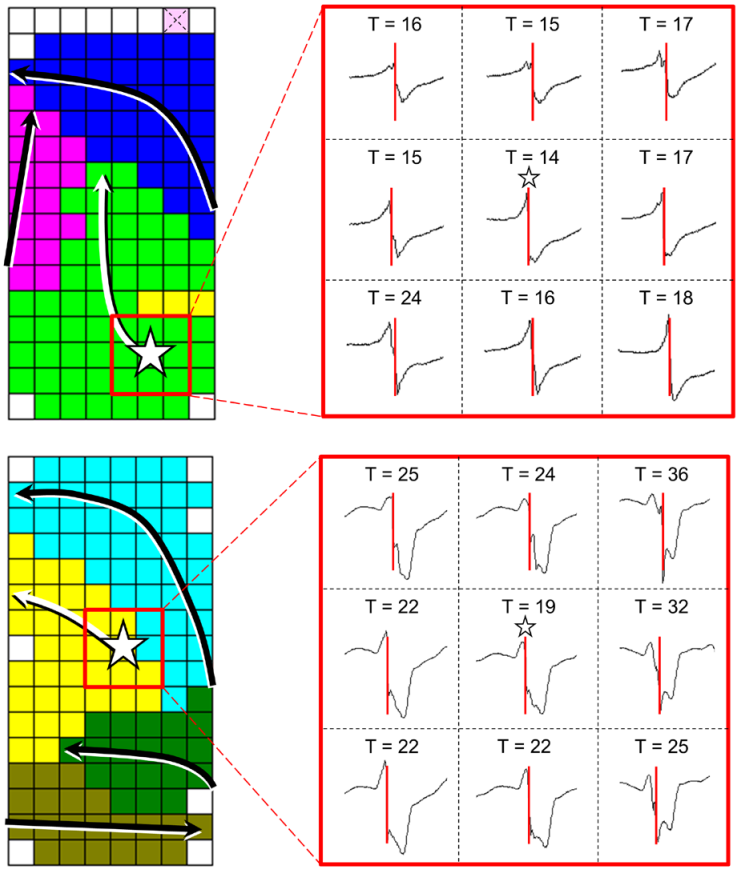

Supplemental Figure 5. Wavemaps demonstrating typical examples of focal fibrillation waves.

Supplemental Table 1. Location of the origin of focal fibrillation waves

Row distance to border	Endocardial focal waves	Epicardial focal waves
2	25%	25%
3	37%	36%
4	38%	39%

Supplemental Table 2. Size of the focal waves

	Endocardial focal waves	Epicardial focal waves
4 electrodes	5.0%	5.6%
5 electrodes	4.5%	5.2%
6 electrodes	3.8%	4.6%

REFERENCES

1. Hoekstra BP, Diks CG, Allessie MA, DeGoede J. Spatial correlation analysis of atrial activation patterns during sustained atrial fibrillation in conscious goats. Arch Physiol Biochem. 2000;108;313-331.
2. Spach MS, Dolber PC. Relating extracellular potentials and their derivatives to anisotropic propagation at a microscopic level in human cardiac muscle. Evidence for electrical uncoupling of side-to-side fiber connections with increasing age. Circ Res. 1986;58:356-371.
3. Spach MS, Kootsey JM. Relating the sodium current and conductance to the shape of transmembrane and extracellular potentials by simulation: effects of propagation boundaries. IEEE Trans Biomed Eng. 1985;32:743-755.
4. Rogers JM, Usui M, KenKnight BH, Ideker RE, Smith WM. Recurrent wavefront morphologies: a method for quantifying the complexity of epicardial activation patterns. Ann Biomed Eng. 1997;25:761-768.
5. Kleber AEG, Rudy Y. Basic Mechanisms of Cardiac Impulse Propagation and Associated Arrhythmias. Physiol Rev. 2004;84:431-488.
6. de Groot NMS, Schalij MJ, Zeppenfeld K, Blom NA, van der Velde ET, van der Wall EE, Schalij MJ. Voltage and activation mapping: how the recording technique affects the outcome of catheter ablation procedures in patients with congenital heart disease. Circulation. 2003;108:2099-2106.
7. Biermann M, Shenasa M, Borggrefe M, Hindricks G, Haverkamp W, Breithard G. Chapter 2. The interpretation of cardiac electrograms, 15-39. From Cardiac Mapping, 2nd edition. From Cardiac Mapping. Shenasa M, Borggrefe M, Breithard G.
8. Biermann M, Borggrefe M, Johna R, Haverkamp W, Shenasa M, Breithardt G. Precision and reproducibility of cardiac mapping. Chapter 8. Precision and reproducibility of cardiac mapping. Chapter 8. 157-186. From Cardiac Mapping, 2nd edition. From Cardiac Mapping. Shenasa M, Borggrefe M, Breithard G.
9. Hertevig EJ, Yuan S, Carlson J, Kongstad-Rasmussen O, Olsson SB. Evidence for electrical remodelling of the atrial myocardium in patients with atrial fibrillation. A study using the monophasic action potential recording technique. Clin Physiol Funct Imaging. 2002;22:8-12
10. Konings KT, Kirchhof CJ, Smeets JR, Wellens HJ, Penn OC, Allessie MA. High-density mapping of electrically induced atrial fibrillation in humans. Circulation. 1994;89:1665-1680.
11. Konings KT, Smeets JL, Penn OC, Wellens HJ, Allessie MA. Configuration of unipolar atrial electrograms during electrically induced atrial fibrillation in humans. Circulation. 1997;95:1231-1241.
12. Allessie MA, de Groot NM, Houben RP, Schotten U, Boersma E, Smeets JL, Crijns HJ. The electropathological substrate of longstanding persistent atrial fibrillation in patients with structural heart disease: longitudinal dissociation. Circ Arrhythm Electrophysiol. 2010;3:606-615.
13. de Groot NMS, Houben RP, Smeets JL, Boersma E, Schotten U, Schalij MJ, Crijns H, Allessie MA. The electropathological substrate of longstanding persistent atrial fibrillation in patients with structural heart disease: epicardial breakthrough. Circulation. 2010;122:1674-1682.
14. Spach MS, Dolber PC, Heidlage JF. Influence of the passive anisotropic properties on directional differences in propagation following modification of the sodium conductance in human atrial muscle. A model of reentry based on anisotropic discontinuous propagation. Circ Res. 1988;62:811-832.